



# Removal of ciprofloxacin via enhancing hydrophilicity of membranes using biochar

Muhammad Zaheer Afzal<sup>1,2</sup> · Said Akbar Khan<sup>3</sup> · Chao Song<sup>1</sup> · Muhammad Imran Irfan<sup>4</sup> · Shu-Guang Wang<sup>1,5</sup>

Received: 5 July 2023 / Accepted: 4 August 2024 / Published online: 12 August 2024  
© The Author(s) 2024

## Abstract

Growing concerns regarding the presence of pharmaceuticals in wastewater necessitate their removal. Membrane filtration offers a promising approach. This study explores the development of biochar incorporated mixed matrix membranes (MMMs) for ciprofloxacin removal from water. Biochar, derived from the pyrolysis of agricultural waste, was blended with polyether sulfone (PES) and polyvinylpyrrolidone in varying ratios. The resulting MMMs exhibited progressively improved properties with increasing biochar content. Notably, membrane M<sub>11</sub>, comprising equal parts PES and biochar, displayed the highest porosity, lowest surface roughness (12.0), and lowest contact angle (31.05°), indicating enhanced hydrophilicity (increased by 58.19% compared to the biochar-free membrane). M<sub>11</sub> effectively removed ciprofloxacin along with three additional antibiotics from different classes. Fourier-transform infrared spectroscopy and X-ray photoelectron spectroscopy analyses corroborated the removal of ciprofloxacin. Furthermore, M<sub>11</sub> demonstrated excellent regenerability, retaining over 57% removal efficiency after four cycles. These findings highlight the potential of M<sub>11</sub> as a sustainable and cost-effective membrane for pharmaceutical removal from wastewater.

**Keywords** Biochar · Membrane filtration · Mixed matrix membrane · Antibiotics · Hydrophilicity

## Introduction

Anthropogenic release of antibiotics into the aquatic environment is of great concern due to their persistent nature and ability to alter ecological processes (Girardi et al. 2011; Zhang et al. 2024, Afzal et al. 2024). Most widely used antibiotics have already been proven genotoxic. Moreover, number of antibiotic resistant bacteria is increasing at an

alarming rate, leading to an enhanced level of gene resistance (Carrales-Alvarado et al. 2014). Ciprofloxacin (CIP) ranks among the top ten pharmaceutical contaminants that disturb the aquatic environment (Ganesan et al. 2019). Moreover, it poses a high risk quotient (RQ > 1) to most sensitive aquatic organisms (Do and Stuckey 2019). The presence of antibiotics in aquatic systems poses a significant threat to human and environmental health. Their detrimental effects

✉ Shu-Guang Wang  
wsg@sdu.edu.cn

Muhammad Zaheer Afzal  
zaheer.afzal82@gmail.com

Said Akbar Khan  
saidakbar2008@yahoo.com

Chao Song  
songchao@sdu.edu.cn

Muhammad Imran Irfan  
imran.irfan@uos.edu.pk

<sup>2</sup> CAS Key Laboratory of Urban Pollutant Conversion, Department of Environmental Science and Engineering, University of Science & Technology of China, Hefei 230026, China

<sup>3</sup> Department of Earth and Environmental Sciences, Bahria University, H-11/4 Campus, Islamabad 44000, Pakistan

<sup>4</sup> Institute of Chemistry, University of Sargodha, Sargodha 40100, Pakistan

<sup>5</sup> WeiHai Research Institute of Industrial Technology of Shandong University, Weihai 264209, China

<sup>1</sup> Shandong Key Laboratory of Water Pollution Control and Resource Reuse, School of Environmental Science and Engineering, Shandong University, Qingdao 266237, China

necessitate the development of efficient and sustainable methods for their removal, ultimately leading to the production of clean water (Shen, et al. 2023; Zhen et al. 2024).

Biochar, due to heterogeneous carboniferous material, plays its role in many environmental remediation, such as wastewater treatment, energy production and soil mitigation (Méndez-Díaz et al. 2010). It has been successfully used to remove organic pharmaceutical compounds and heavy metals (Qian et al. 2016) from aqueous solutions. However, bare biochar has the problem of difficulty in precise distribution of its particles when used on a large-scale plant and difficulty of its separation for regeneration after treatment.

Membrane filtration, a general way of treating wastewater in several industries worldwide due to its low manufacturing cost and large area, may be a potential solution for separation of organic pollutants from water (Yue et al. 2020). Polyether sulfone (PES), a polymeric material, is frequently used in synthesis of membranes due to excellent thermal and chemical resistance (Arkhangelsky, et al. 2007; Wang et al. 2018). But PES is hydrophobic in nature and polyvinylpyrrolidone (PVP) is added to increase the hydrophilicity of membrane because hydrophilic surface of membrane is advantageous in enhancing water permeate flux and to mitigate membrane fouling. Crucially, this study addresses the persistent challenge of membrane fouling, a major bottleneck in wastewater treatment. Conventional membranes are susceptible to fouling by organic contaminants, significantly reducing their filtration efficiency. However, this research leverages the unique properties of biochar. Its inherent surface functional groups, as highlighted by Sima et al. (2017), enhance membrane hydrophobicity, a key factor in mitigating fouling. By incorporating biochar into the membrane matrix, we propose a novel and potentially transformative strategy (win–win) for wastewater treatment. Moreover, conventional membranes offer filtration, they lack the ability to effectively remove pharmaceutical contaminants like ciprofloxacin. This limitation necessitates innovative solutions. Our study presents a groundbreaking approach using biochar incorporated mixed matrix membranes (MMMs). MMMs represent a paradigm shift in membrane technology, transcending the limitations of traditional membranes. By strategically incorporating biochar, a readily available, sustainable material, into the polymeric matrix, we create a novel system with dual functionalities: size-exclusion filtration from the membrane itself and enhanced adsorption from the biochar. This synergistic combination offers unparalleled potential for ciprofloxacin removal. Unlike conventional membranes that solely rely on filtration, our MMMs leverage the adsorptive properties of biochar to capture these contaminants more efficiently (Mukherjee et al. 2016). This research paves the way for a new generation of MMMs specifically designed to address the growing challenge of pharmaceutical residues in wastewater treatment. This approach not only addresses

the critical issue of pharmaceutical removal but also offers a sustainable solution by utilizing a waste product (agricultural waste) as a functional component of the membrane. MMMs possess the advantageous dual functionality of both adsorption and filtration, occurring simultaneously within the membrane structure. This unique capability has led to demonstrably enhanced membrane performance compared to traditional membranes (Chu et al. 2017).

In this study, we fabricated MMM using controlled composition of PES, PVP and biochar with uniform loading for separation of CIP. Characterization analyses of prepared membranes were performed by Scanning electron microscopy (SEM), atomic force microscopy (AFM), contact angle measurement, Fourier-transform infrared attenuated total reflection (FTIR-ATR) and X-ray photoelectron spectroscopy (XPS). Main aims of this study were to construct biochar into membrane to minimize fouling and to enhance the separation efficiency. Determination of water flux and CIP removal was performed by using dead-end filtration assembly. Finally, membrane was regenerated for repeated removal of CIP.

## Materials and methods

### Materials

PES was purchased from Sigma Aldrich. Ciprofloxacin, tetracycline (TET), ceftriaxone sodium (CTA), chloramphenicol (CAP), PVP and dimethyl acetamide (DMAc > 98%), were purchased from Aladdin Chemicals Reagent Company (Shanghai, China). All substances were used without any refining. Biochar was prepared with the procedure mentioned in our previous studies (Afzal et al. 2019, 2018). Briefly, small pieces of peels of grapefruit were burnt in a muffle furnace at 450 °C for 15 min followed by grinding and sieving through 0.3 mm.

### Preparation of biochar/PES membranes

Biochar-based PES membranes were prepared by a well-known thermal phase inversion (TPI) method. Specifically, four solutions were prepared in different beakers by dissolving 1.70 g PES and 0.1 g PVP in 8.72 mL of DMAc in each of beaker while continuous stirring at 60 °C until homogeneous solution was achieved. One of the above prepared solution was proceeded without any addition and the membrane prepared from this solution was named as  $M_0$ . Whereas, in each of the remaining three PES solution, 1.70 g, 0.85 g and 0.425 g of biochar were added to make membranes of PES: biochar ratio of 1:1, 2:1 and 4:1,

which were then named as  $M_{11}$ ,  $M_{21}$  and  $M_{41}$ , respectively. Solutions were further stirred at 60°C for 24 h followed by venting in a vacuum oven at 50 °C for 4 h. The solutions were then shaped into membrane glass plates with a suitable applicator to maintain a uniform thickness of 150  $\mu\text{m}$ . Casted solutions along with glass plates were instantly transferred to coagulation bath containing deionized water (DI) water. After peeling off the membranes from glass plates, they were transferred into DI water again for 24 h to remove any undissolved PVP.

## Characterization of membranes

Surface and cross sectional morphologies of membranes, before filtration, were characterized with SEM (QUANTA FEG 250; FEI, Holland). For SEM cross sectional analysis, brittle fracturing of membranes was done with liquid nitrogen before capturing of SEM images. To evaluate the surface roughness and morphology of membranes, AFM (NanoManVS, UK) was used. Moreover, membranes, before and after filtration, were subjected to different characterization analyses. FTIR-ATR spectroscopic measurements (Perkin Elmer FTIR spectrometer (Frontier Optica)) to investigate the surface functional groups. Hydrophilic/hydrophobic properties were assessed by measuring water contact angle using DSA30E Kruss Drop shape analyzer, (GmbH, Germany). XPS (PHYSICAL ELECTRONICS/PHI 5300, USA) was applied for materials surface characterization. Gravimetric method was used to measure porosity ( $\epsilon$ ) of membrane, as mentioned in Eq. 1 (Vatanpour et al. 2012).

$$\epsilon = \frac{\omega - \omega'}{A * l * d_w} \quad (1)$$

where  $\omega$  and  $\omega'$  are weight of the wet and dried membranes;  $A$  is effective area of membrane ( $\text{m}^2$ ),  $d_w$  denotes water density ( $0.998 \text{ g/cm}^3$ ) and  $l$  is the membrane thickness ( $m$ ).

Average pore radius ( $r_m$ ) was measured with the following Guerout–Elford–Ferry equation (Hamid et al. 2011).

$$r_m = \sqrt{\frac{(29 - 1.75\epsilon)8\eta l Q}{\epsilon A \Delta P}} \quad (2)$$

where  $\eta$  is viscosity of water ( $8.9 \times 10^{-4} \text{ Pa.s}$ );  $Q$  is volume of the permeate water per unit time ( $\text{m}^3/\text{s}$ );  $\Delta P$  is operational pressure (0.1 MPa).

Specific surface area (SSA) of the prepared membranes was calculated by applying following equation (Lowell et al. 2012).

$$\text{SSA} = \frac{2 * \epsilon}{r_m} \quad (3)$$

where  $\epsilon$  is porosity (%) and  $r_m$  is pore radius ( $m$ ).

## Filtration experiments

To investigate the membrane's filtration performance, a laboratory scale dead-end filtration set up was utilized, using a circular piece of membranes with effective area of  $4.91 \text{ cm}^2$ . The dead-end filtration assembly consists of aeration tank connected to nitrogen gas cylinder on one end and to stirring cell on another end. Also, there is a filtrate collector, which is placed on an electric balance. To measure water flux, feed solution (DI water) was forced to pass through membrane by applying 0.1 MPa pressure of nitrogen gas for 30 min. Increase in weight of filtered water was used to calculate water flux  $J$  ( $\text{L/m}^2\text{h}$ ) using Eq. 4 (Ghaffar et al. 2018).

$$J = \frac{\Delta m}{\rho * A * t} \quad (4)$$

$J$  represents water flux in  $\text{L/m}^2\text{h}$ ;  $\Delta m$  is weight of filtered water;  $\rho$  is water density ( $0.998 \text{ g/mL}$ );  $A$  represents effective area of membrane ( $\text{m}^2$ );  $t$  stands for time ( $h$ ).

To check membrane efficiency for CIP removal, its solution of  $10 \text{ mg/L}$  was used as feed solution and forced to pass through membrane for 30 min. Then, absorbances of passed solutions were measured at a wavelength of  $276 \text{ nm}$  with UV/Vis spectrophotometer (UV5100, China). Removal efficiency (rejection) was calculated with following Eq. 5.

$$R\% = \frac{C_0}{C_e} * 100 \quad (5)$$

where  $C_0$  is pre-filtration concentration of ciprofloxacin ( $\text{mg/L}$ ), and  $C_e$  is post filtration concentration of ciprofloxacin ( $\text{mg/L}$ ).

Similarly, feed solutions of other three antibiotics, TET, CTA and CAP, at the same concentrations were also subjected to filtration, and their absorbances were measured at  $360 \text{ nm}$ ,  $240 \text{ nm}$ , and  $277 \text{ nm}$ , respectively. To regenerate membrane, used membrane was put into  $0.1 \text{ M HCl}$  solution for 30 min to desorb ciprofloxacin for repeated filtration. At beginning of each measurement, either flux or pollutant filtration, membranes were cleaned via passing DI water under nitrogen pressure of  $0.15 \text{ MPa}$  for 30 min.

## Results and discussion

### Morphology and structure of membranes

PES/biochar membranes were fabricated by insertion of biochar into bulk PES solution. The colors of membranes became darker with increased ratio of biochar (Fig. 1a).

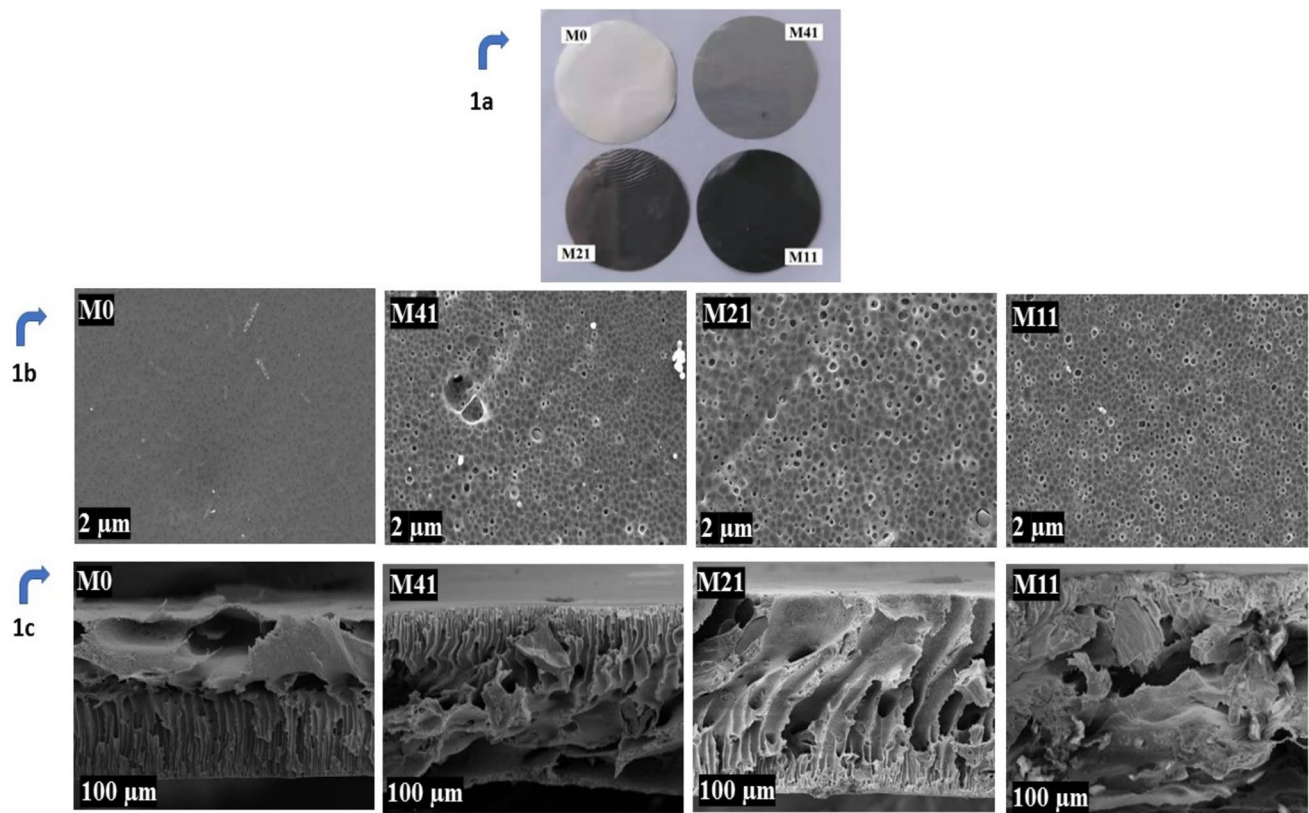


**Fig. 1** **a** Naked eye appearance of the prepared membranes; **b** SEM images of the prepared membranes; **c** Cross sectional SEM images of the prepared membranes

To get through the exact structures of membranes, membranes surface and their cross sections were investigated with SEM. The morphologies of prepared membranes significantly changed with different ratio of biochar. As shown in Fig. 1b, more pores are generated with the increasing biochar ratio. The increased ration of biochar inclines to cumulate with each other, resulting in suppressed pores. Cross sectional images of prepared membranes clearly showed the spongy structure with invariant dispersion of biochar which ensures the physical strength of membranes and uniform distribution of flow through it. Thickness of membranes cross sections increased with increase in biochar ratio and membranes  $M_{21}$  and  $M_{11}$  were found to have longer pore channels and more abundant.

Roughness of membrane was examined with AFM, which was performed by scanning of  $8\ \mu\text{m} \times 8\ \mu\text{m}$  of membrane's surface (Fig. 2). Dark areas exemplify membrane's pore/valley and that of bright regions indicate the highest site of membrane's surface. Several peaks on surface of  $M_0$  were detected, indicating the roughness of high degree, and the roughness decreased with the increasing ratio of biochar. Moreover, decrease in Ra value with increase in biochar ratio is another evidence of decrease in roughness.  $M_0$ ,  $M_{41}$ ,  $M_{21}$  and  $M_{11}$  had Ra values at 39.2, 25.0, 15.0 and

12.0, respectively. Smooth surface topography of membrane decreases its surface area, which leads to reduction in fouling of membrane and enhances its ability to remove contaminants (Li et al. 2018; Wu et al. 2020).

### Properties of membranes

In Table 1, porosity and pore radius were increased with increasing biochar ratio, which in turn improved membrane's permeability (Tiraferri et al. 2011). Porosity of the membranes were calculated to be 48.6% ( $M_0$ ), 51.6% ( $M_{41}$ ), 62.4% ( $M_{21}$ ) and 68.9% ( $M_{11}$ ). Whereas, pore radius was 90.61 nm ( $M_0$ ), 232.46 nm ( $M_{41}$ ), 248.07 nm ( $M_{21}$ ) and 266.96 nm ( $M_{11}$ ). Increase in pore radius increases water flux. As remaining parameters of Eq. 2 are kept constant, pore radius becomes directly proportional to square root of flux (Wang et al. 2013).

Hydrophilic characteristics of prepared membranes were characterized by measuring water contact angle. As shown in Fig. 3, contact angle of  $M_0$  was 74.26, which continuously decreased upon increase in biochar content.  $M_{41}$ ,  $M_{21}$  and  $M_{11}$  had contact angles of 62.86, 45.84 and 31.05, respectively. This corresponds to increase in hydrophilic nature upon increase in biochar content and the successive

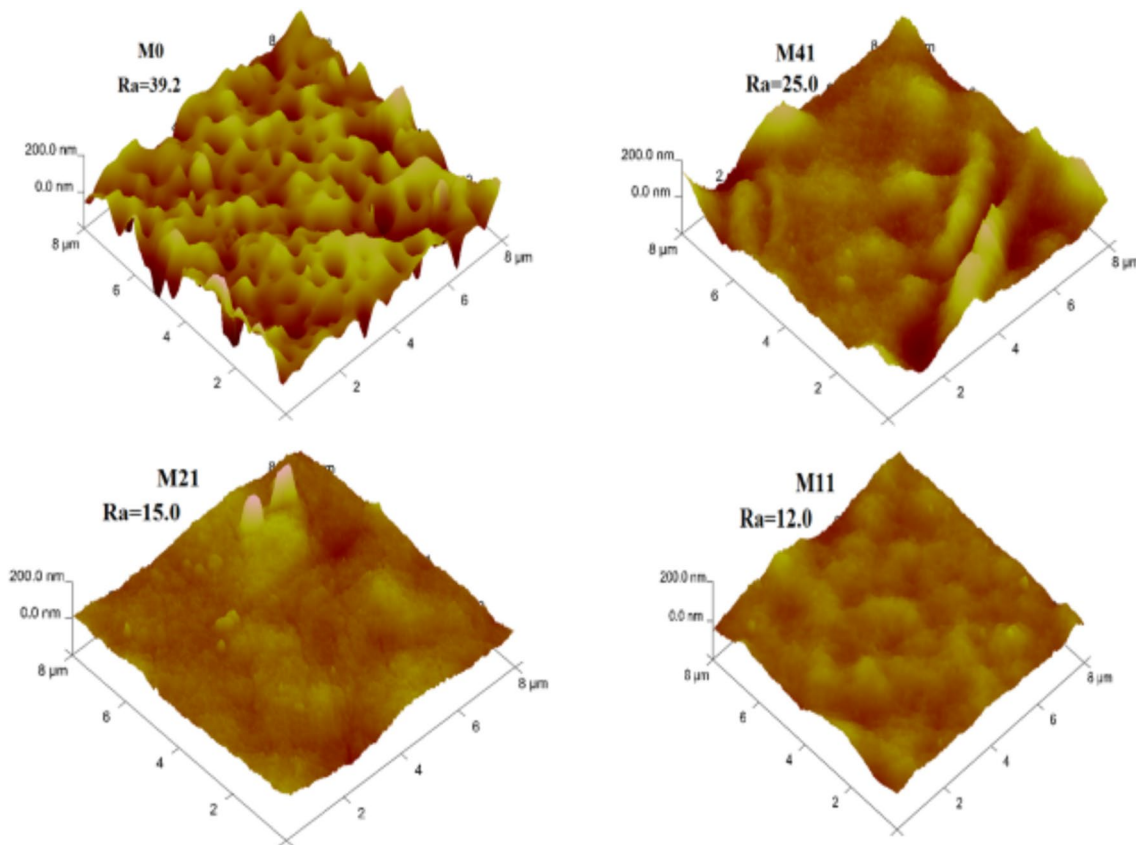


Fig. 2 AFM images of the prepared membranes 100 μm

Table 1 Different characterization properties of the prepared membranes

Membrane	Contact angle (°)	Ra	Porosity (%)	Pore radius (nm)	Specific surface area (m <sup>2</sup> /m <sup>3</sup> )
M <sub>0</sub>	74.26	39.2	48.6	90.6	10.73*10 <sup>6</sup>
M <sub>41</sub>	62.86	25.0	51.6	232.5	4.44*10 <sup>6</sup>
M <sub>21</sub>	45.84	15.0	62.4	248.1	5.03*10 <sup>6</sup>
M <sub>11</sub>	31.05	12.0	68.9	267.0	5.16*10 <sup>6</sup>

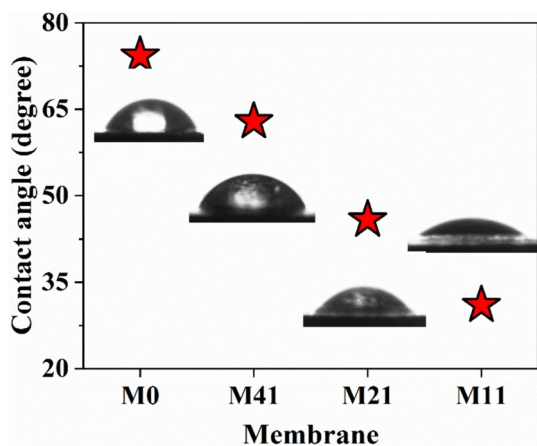
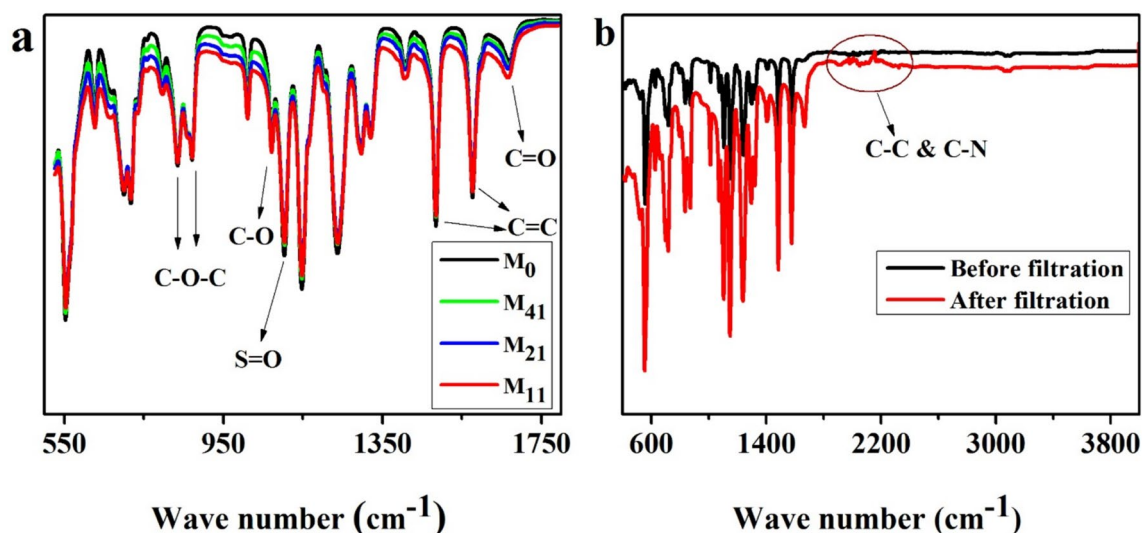


Fig. 3 Contact angles of the prepared membranes

improvement in hydrophilicity were 15.35%, 38.27% and 58.19%, respectively. It is because of the presence of functional groups on biochar’s surface such as -OH and -CH. These results indicate the excellent hydrophilicity of biochar.

Figure 4a displays the FTIR spectra from 1800 cm<sup>-1</sup> to 500 cm<sup>-1</sup> for all the prepared membranes (M<sub>0</sub>, M<sub>41</sub>, M<sub>21</sub> and M<sub>11</sub>). Peaks at 700 and 717 cm<sup>-1</sup> are due to aromatic sulfo group present in PES, those at 835 and 871 could be assigned to C–O–C bond (Afzal et al. 2022a). Peaks at 1071 and 1103 cm<sup>-1</sup> could be designated to C–O group and S=O group, respectively. Peak at 1297 cm<sup>-1</sup> was attributed to asymmetric stretching of S=O bonds and symmetrical stretching vibrations of the same bond was observed at 1147 cm<sup>-1</sup> (Huang et al. 2017). Peak at 1237 cm<sup>-1</sup> represents the C–O–C stretching vibrations of PES backbone material



**Fig. 4** FTIR spectra of: **a** all the prepared membranes; **b**  $M_{11}$  before and after filtration

**Table 2** Flux and rejection efficiencies of the prepared membranes

Membrane	Flux ( $L/m^2h$ )		Rejection (%)
	Water	CIP	
$M_0$	434	48	10.3
$M_{41}$	518	335	25.8
$M_{21}$	761	542	77.9
$M_{11}$	790	583	95.2

(Hanafi et al. 2016). Peaks at 1485 and 1577  $cm^{-1}$  were attributed to C=C bond (Rabiller-Baudry et al. 2015). PVP shows its presence in the form of peak at 1668  $cm^{-1}$  which was due to C=O vibration of the PVP amide group (Fu and Zhang 2019). Whereas Fig. 4b shows FTIR spectra of  $M_{11}$  before and after filtration. It is evident from the FTIR analyses that membrane, after filtration, exhibited new peaks between 2400 and 1800  $cm^{-1}$ . According to Mao et al. (Mao et al. 2016), peaks in this region are indication of creation of bonds of C–C and C–N. It further indicates the chemical adsorption of CIP on membrane surface.

### Performance of membranes

Performances of all four manufactured membranes were tested with water flux measurements and ciprofloxacin rejection using dead-end filtration system. As listed in Table 2, water flux of all prepared membranes was higher than that of their respective ciprofloxacin flux. It may be because of blockage of pores and engagement of functional groups on membrane's surface by ciprofloxacin. Water flux of  $M_0$  was 434 LMH, which was increasing with biochar content i.e.,  $M_{41}$ ,  $M_{21}$  and  $M_{11}$  had water flux of 518, 761 and 790,

respectively. Increase in water flux with biochar content may possibly be due to hydrophilic nature of biochar, which allows its nanochannels to enter more water molecules, resulting in increase in water flux (Heiranian et al. 2015). Smooth surface of membranes, with increasing biochar content, can be another reason of high flux because of hydraulic resistance (Wang et al. 2017). Moreover, it is visible from Fig. 6a that decrease in water/CIP flux is negligible with passage of time, confirming the least fouling of membranes.

Figure 5 showcases the X-ray photoelectron spectroscopy (XPS) analysis of  $M_{11}$  membranes before and after filtration, providing compelling evidence of ciprofloxacin (CIP) removal through interaction with the membrane surface. The C1s core spectra reveal a critical shift after filtration. Prior to filtration, two dominant peaks were observed: one at 284.53 eV corresponding to C–C, C=C (aromatic and aliphatic carbons), and another at 285.54 eV indicative of C–O–C bonds. However, following filtration, a new peak emerges at 286.86 eV, which can be attributed to O–C=O bonds. This newly formed peak signifies the interaction between CIP and the carbonyl groups present on the membrane surface, potentially through hydrogen bonding or other mechanisms. Similarly, the N1s core spectra corroborate this interaction. The pre-filtration spectra exhibit two peaks at 399.48 eV and 399.95 eV, corresponding to N–C=O and C–NH<sub>2</sub> bonds, respectively. Interestingly, after filtration, a new peak appears at 398.93 eV, indicative of N–H bonds. The presence of this new peak suggests the formation of new bonds between the nitrogen atom in CIP and functional groups on the membrane surface, likely involving amine groups. In essence, the creation of these new peaks in both C1s and N1s spectra provides strong evidence of chemical interaction between CIP and the functional groups present

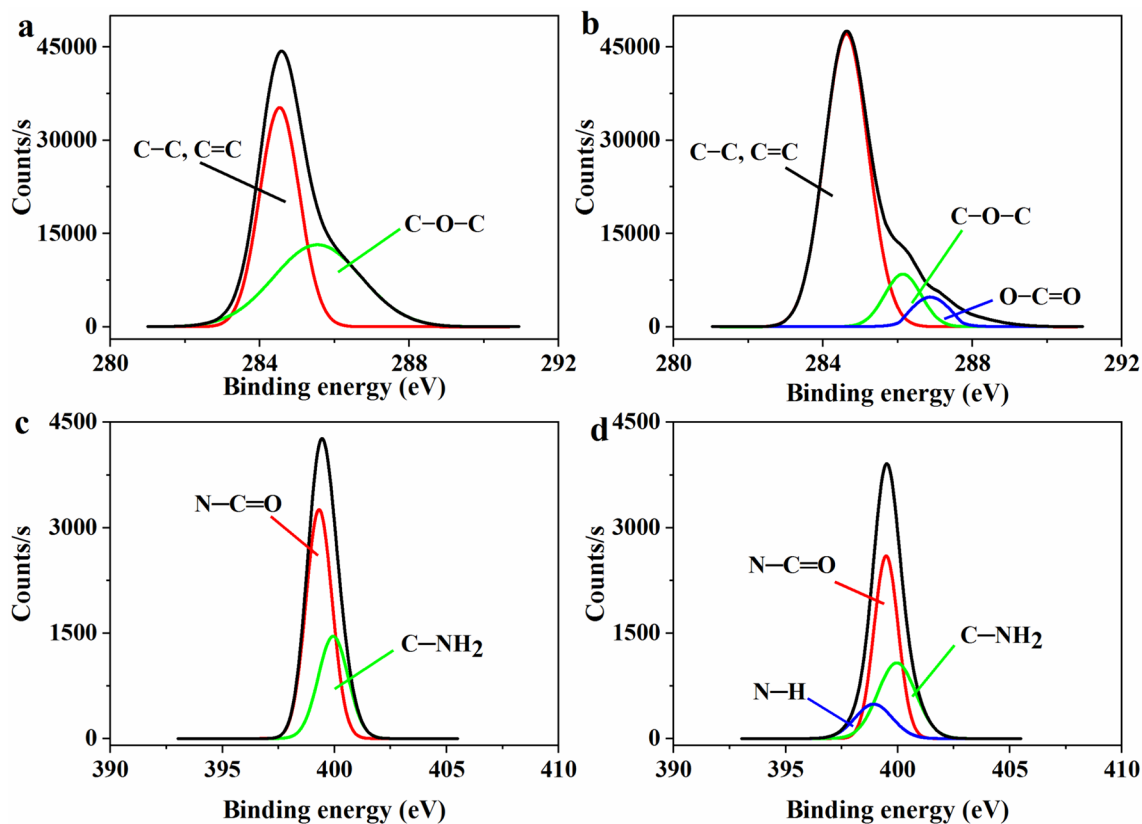


**Fig. 5** C 1s core spectra of  $M_{11}$ : **a** before filtration; **b** after filtration; N 1s core spectra of  $M_{11}$ : **c** before filtration; **d** after filtration

on the M11 membrane surface. Our previous study (Afzal et al. 2019) also exhibited the similar phenomenon. So, this XPS analysis reinforces the effectiveness of the biochar incorporated MMMs in removing ciprofloxacin from water through a combination of adsorption and filtration mechanisms.

As mentioned in Fig. 6, rejection of ciprofloxacin significantly improved with increase in biochar content.  $M_{11}$  had the highest rejection of 95.19% which was substantially higher than 77.92% ( $M_{21}$ ), 25.76% ( $M_{41}$ ) and 10.27% ( $M_0$ ). It may be due to superior adsorption behavior of biochar. The increase in membrane hydrophilicity by biochar also enhances the membrane's wettability (Zhao et al. 2013; Wang et al. 2019), which creates more opportunities for ciprofloxacin collision with surface of membrane. Therefore, a membrane with higher biochar content can adsorb more ciprofloxacin leading to more rejection than that of with low or zero biochar content.

Along with ciprofloxacin, three other antibiotics, TET, CTA, and CAP, were filtered through  $M_{11}$ , and their rejection was monitored.  $M_{11}$  also showed great interaction with these antibiotics, and rejection of these antibiotics was quite enough i.e., 82.39% (TET), 88.61% (CTA) and 57.63% (CAP). These result suggest that  $M_{11}$  can be used for the

removal of wide range of antibiotics. Overall, biochar was helpful in constructing porous membranes of smooth surface topography, increased pore radii, and increased hydrophilicity. It in turn increased the efficiencies of membranes in terms of increased flux and more rejection ability for CIP confirmed with different characterization analyses. Building upon previous research, the data presented in Table 3 indicate that  $M_{11}$  exhibits superior rejection efficiency for contaminants of emerging concern specifically for CIP. This observation further strengthens the notion that  $M_{11}$  possesses exceptional capabilities for the removal of CIP and other organic micro-pollutants.

### Filtration mechanism

Our analysis of the data helped us identify the most likely way the filtration mechanism, which can be described as below:

#### Size exclusion

The Ra value of 12.0 nm suggests a relatively smooth membrane surface. This allows for size-based separation. Moreover, pore size falls within the typical range for ultrafiltration

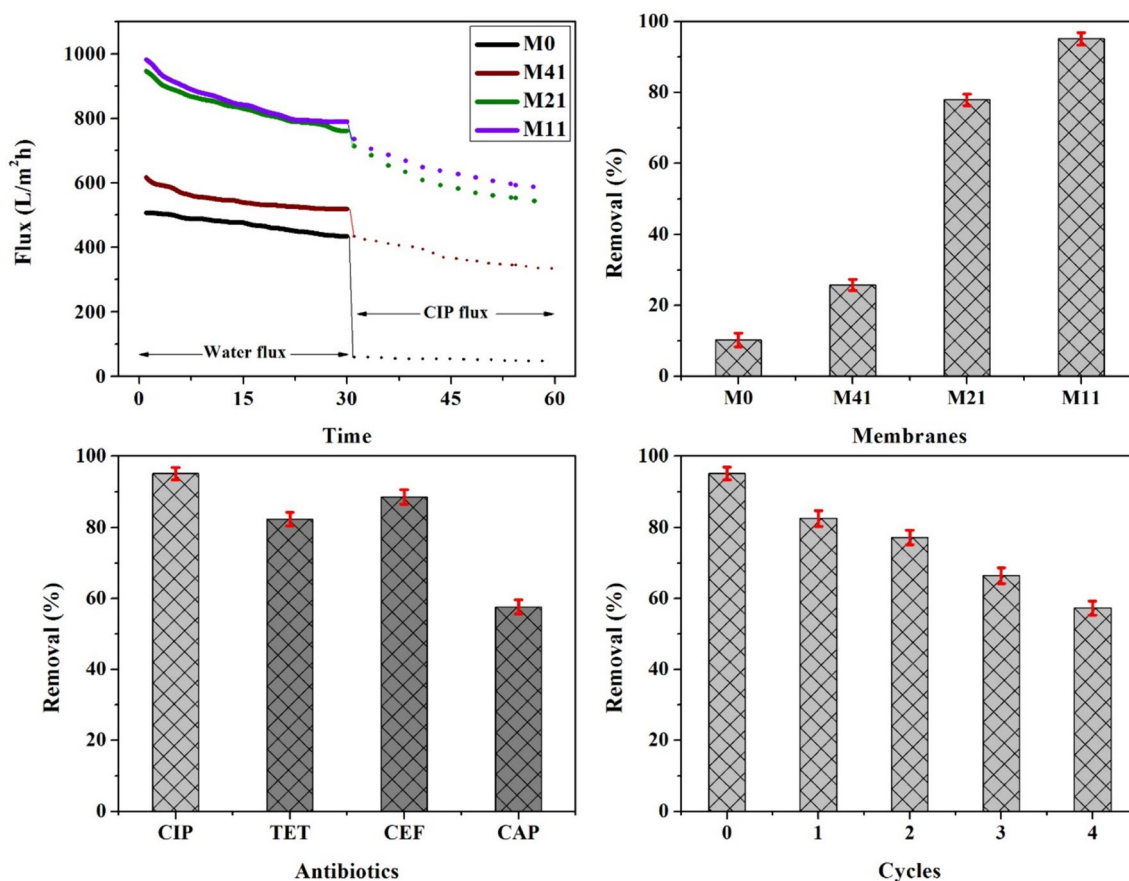


**Fig. 6** a Water and ciprofloxacin flux; b removal efficiencies of all the membranes for ciprofloxacin; c removal efficiency of M<sub>11</sub> for different antibiotics; d removal efficiency of M<sub>11</sub> after different regeneration cycles

**Table 3** Comparison of the rejection efficiency of the prepared membrane with previously reported studies about antibiotics removal

Membrane material	Pollutant	Rejection (%)	References
PES/PVP/GO-TiO <sub>2</sub>	Ciprofloxacin	58.0	(Goyat et al. 2024)
PVDF/g-C <sub>3</sub> N <sub>4</sub> /TiO <sub>2</sub>	Sulfamethoxazole	72.8	(Liu et al. 2023)
PVDF/CeO <sub>2</sub> @GO-COOH	Sulfanilamide	79.5	(Utomo et al. 2023)
PSU/MIL-125-NH <sub>2</sub> (Ti)	Fluoxetine hydrochloride	84.5	(Rad et al. 2024)
CeO <sub>2</sub> @CNT	Carbamazepine	89.4	(Ma et al. 2023)
PES/PVP/biochar	Ciprofloxacin	95.2	This study

membranes, which can effectively reject larger particles like bacteria, viruses, and some macromolecules, while allowing water to pass through. Also, porosity of 68.9% is a high value, meaning a significant portion of the membrane volume is occupied by pores. This allows for a larger volume of water to pass through the membrane.

### Adsorption

Biochar, incorporated into the membrane, is known for its high adsorption capacity. When ciprofloxacin comes in contact with the biochar within the membrane, it can get

adsorbed onto the biochar's surface through various mechanisms like electrostatic interactions,  $\pi$ - $\pi$  interactions, or hydrogen bonding (Afzal et al. 2022b). This phenomenon contributes to ciprofloxacin rejection.

### Hydrophilicity

The low contact angle of 31.05° indicates a highly hydrophilic membrane. This means the membrane surface has a strong affinity for water. As water molecules preferentially interact with the membrane surface, they form a hydration layer that hinders the passage of hydrophobic contaminants



like ciprofloxacin. This creates a repulsive force between the membrane and the contaminant, further enhancing rejection. Also, porosity of 68.9% is a high value, meaning a significant portion of the membrane volume is occupied by pores. This allows for a larger volume of water to pass through the membrane.

## Regeneration of membrane

Regeneration experiments were performed to check the sustainability of  $M_{11}$  and its economic value. It was done by desorbing, which is a utile to regenerate used membranes (Huang et al. 2016). Membrane was suspended in 0.1 M HCl for 30 min to detach ciprofloxacin from it before using it again for ciprofloxacin rejection. We executed four rejection/desorption cycles during which the rejection efficiency of membrane decreased in each of the successive cycle which may be owing to the decline in strength of different functional groups and pores on membrane's surface. While the regeneration experiments achieved a rejection efficiency of over 57% even in the 4th cycle, indicating promising reusability of  $M_{11}$ , further optimization might be necessary to maximize its regeneration potential for extended lifespans. Nonetheless, compared to single-use membranes,  $M_{11}$  offers a more sustainable and potentially economical solution for ciprofloxacin removal from water.

## Conclusion

In this study, we prepared 4 different membranes ( $M_0$ ,  $M_{41}$ ,  $M_{21}$  and  $M_{11}$ ) via mixing different ratios of biochar in PES and PVP for filtration of ciprofloxacin from water.  $M_{11}$  was found to be more acceptable as it has highest water/ciprofloxacin flux (790/595), highest porosity (68.9), least contact angle (31.05) and least roughness (12.0). Ciprofloxacin rejection by  $M_{11}$  was 95.19%. It also showed good rejection for 3 other antibiotics i.e., TET (82.39%), CTA (88.61%) and CAP (57.63%). Removal capability of  $M_{11}$  was confirmed with FTIR and XPS analyses in which some new peaks were observed.  $M_{11}$  was also regenerated 4 times and it showed removal efficiency of more than 57% in last cycle. These results proved  $M_{11}$ , a sustainable and economical for filtration of ciprofloxacin from water. Hence, this study reveals the effectiveness of biochar in enhancing hydrophilic nature of membranes. The influence of real wastewater composition, particularly the presence of diverse organic matter, on membrane fouling and long-term performance necessitates further investigation. Additionally, optimization of biochar incorporation ratios and exploration of biochar derived from various feedstock hold promise for enhanced membrane performance and broader applicability across a wider range of contaminants.

**Acknowledgements** This research was supported by the National Natural Science Foundation of China (U20A20146).

**Funding** This research was funded by the National Natural Science Foundation of China (Grant number: U20A20146).

**Data availability** The data used to support the findings of this study are included within the article and supplementary material.

## Declarations

**Conflict of interest** The authors have no relevant financial or non-financial interests to disclose.

**Ethical approval** This study did not involve any vivo experiments and does not apply to any ethical approval necessary.

**Open Access** This article is licensed under a Creative Commons Attribution-NonCommercial-NoDerivatives 4.0 International License, which permits any non-commercial use, sharing, distribution and reproduction in any medium or format, as long as you give appropriate credit to the original author(s) and the source, provide a link to the Creative Commons licence, and indicate if you modified the licensed material. You do not have permission under this licence to share adapted material derived from this article or parts of it. The images or other third party material in this article are included in the article's Creative Commons licence, unless indicated otherwise in a credit line to the material. If material is not included in the article's Creative Commons licence and your intended use is not permitted by statutory regulation or exceeds the permitted use, you will need to obtain permission directly from the copyright holder. To view a copy of this licence, visit <http://creativecommons.org/licenses/by-nc-nd/4.0/>.

## References

- Afzal MZ, Sun X-F, Liu J, Song C, Wang S-G, Javed A (2018) Enhancement of ciprofloxacin sorption on chitosan/biochar hydrogel beads. *Sci Total Environ* 639:560–569
- Afzal MZ, Yue R, Sun X-F, Song C, Wang S-G (2019) Enhanced removal of ciprofloxacin using humic acid modified hydrogel beads. *J Colloid Interface Sci* 543:76–83
- Afzal MZ, Zu P, Zhang C-M, Guan J, Song C, Sun X-F, Wang S-G (2022a) Sonocatalytic degradation of ciprofloxacin using hydrogel beads of TiO<sub>2</sub> incorporated biochar and chitosan. *J Hazard Mater* 434:128879
- Afzal MZ, Hameed S, Mohiuddin M, Abbasi A (2022b) Simultaneous adsorptive removal of three fluoroquinolones using humic acid modified hydrogel beads. *Environ Sci Pollut Res*. <https://doi.org/10.1007/s11356-022-23855-3>
- Afzal MZ, Zha M, Zhang H, Ma C, Li H, Wang Y (2024) Copper-incorporated zinc manganite as a novel catalyst for activating peroxymonosulfate in the degradation of tetracycline. *Sep Purif Technol* 354:128673
- Arkhangelsky E, Kuzmenko D, Gitis V (2007) Impact of chemical cleaning on properties and functioning of polyethersulfone membranes. *J Membr Sci* 305:176–184
- Carrales-Alvarado DH, Ocampo-Pérez R, Leyva-Ramos R, Rivera-Utrilla J (2014) Removal of the antibiotic metronidazole by adsorption on various carbon materials from aqueous phase. *J Colloid Interface Sci* 436:276–285

- Chu KH, Fathizadeh M, Yu M, Flora JRV, Jang A, Jang M, Park CM, Yoo SS, Her N, Yoon Y (2017) Evaluation of removal mechanisms in a graphene oxide-coated ceramic ultrafiltration membrane for retention of natural organic matter pharmaceuticals, and inorganic salts. *Acs Appl Mater Interfaces* 9:40369–40377
- Do MT, Stuckey DC (2019) Fate and removal of ciprofloxacin in an anaerobic membrane bioreactor (AnMBR). *Bioresour Technol* 289:121683
- Fu W, Zhang W (2019) Chemical aging and impacts on hydrophilic and hydrophobic polyether sulfone (PES) membrane filtration performances. *Polym Degrad Stab* 168:108960
- Ganesan S, Amirthalingam M, Arivalagan P, Govindan S, Palanisamy S, Lingassamy AP, Ponnusamy VK (2019) Absolute removal of ciprofloxacin and its degraded byproducts in aqueous solution using an efficient electrochemical oxidation process coupled with adsorption treatment technique. *J Environ Manag* 245:409–417
- Ghaffar A, Zhu X, Chen B (2018) Biochar composite membrane for high performance pollutant management: fabrication, structural characteristics and synergistic mechanisms. *Environ Pollut* 233:1013–1023
- Girardi C, Greve J, Lamshoef M, Fetzer I, Miltner A, Schaeffer A, Kaestner M (2011) Biodegradation of ciprofloxacin in water and soil and its effects on the microbial communities. *J Hazard Mater* 198:22–30
- Goyat R, Singh J, Umar A, Saharan Y, Ibrahim AA, Akbar S, Baskoutas S (2024) Synthesis and characterization of nanocomposite based polymeric membrane (PES/PVP/GO-TiO<sub>2</sub>) and performance evaluation for the removal of various antibiotics (amoxicillin, azithromycin & ciprofloxacin) from aqueous solution. *Chemosphere* 353:141542
- Hamid NAA, Ismail AF, Matsuura T, Zularisam AW, Lau WJ, Yuliwati E, Abdullah MS (2011) Morphological and separation performance study of polysulfone/titanium dioxide (PSF/TiO<sub>2</sub>) ultrafiltration membranes for humic acid removal. *Desalination* 273:85–92
- Hanafi Y, Loulergue P, Ababou-Girard S, Meriadec C, Rabiller-Baudry M, Baddari K, Szymczyk A (2016) Electrokinetic analysis of PES/PVP membranes aged by sodium hypochlorite solutions at different pH. *J Membr Sci* 501:24–32
- Heiranian M, Farimani AB, Aluru NR (2015) Water desalination with a single-layer MoS<sub>2</sub> nanopore. *Nat Commun*. <https://doi.org/10.1038/ncomms9616>
- Huang X, Liu Y, Liu S, Tan X, Ding Y, Zeng G, Zhou Y, Zhang M, Wang S, Zheng B (2016) Effective removal of Cr(VI) using beta-cyclodextrin-chitosan modified biochars with adsorption/reduction bifunctional roles. *RSC Adv* 6:94–104
- Huang J, Yang H, Chen M, Ji T, Hou Z, Wu M (2017) An infrared spectroscopy study of PES/PVP blend and PES-g-PVP copolymer. *Polym Testing* 59:212–219
- Li M-N, Sun X-F, Wang L, Wang S-Y, Afzal MZ, Song C, Wang S-G (2018) Forward osmosis membranes modified with laminar MoS<sub>2</sub> nanosheet to improve desalination performance and antifouling properties. *Desalination* 436:107–113
- Liu H, Zhang H, Dong X, Wu C, Lichtfouse E (2023) Removal of antibiotics from black water by a membrane filtration-visible light photocatalytic system. *J Water Process Eng* 53:103605
- Lowell S, Shields JE, Thomas MA, Thommes M (2012) Characterization of porous solids and powders: surface area, pore size and density. Springer Science & Business Media, Netherlands
- Ma Q, Chu Y, Ni X, Zhang J, Chen H, Xu F, Wang Y (2023) CeO<sub>2</sub> modified carbon nanotube electrified membrane for the removal of antibiotics. *Chemosphere* 310:136771
- Mao H, Wang S, Lin J-Y, Wang Z, Ren J (2016) Modification of a magnetic carbon composite for ciprofloxacin adsorption. *J Environ Sci China* 49:179–188
- Méndez-Díaz JD, Prados-Joya G, Rivera-Utrilla J, Leyva-Ramos R, Sánchez-Polo M, Ferro-García MA, Medellín-Castillo NA (2010) Kinetic study of the adsorption of nitroimidazole antibiotics on activated carbons in aqueous phase. *J Colloid Interface Sci* 345:481–490
- Mukherjee R, Bhunia P, De S (2016) Impact of graphene oxide on removal of heavy metals using mixed matrix membrane. *Chem Eng J* 292:284–297
- Qian L, Zhang W, Yan J, Han L, Gao W, Liu R, Chen M (2016) Effective removal of heavy metal by biochar colloids under different pyrolysis temperatures. *Biores Technol* 206:217–224
- Rabiller-Baudry M, Bouzin A, Hallery C, Girard J, Leperoux C (2015) Evidencing the chemical degradation of a hydrophilised PES ultrafiltration membrane despite protein fouling. *Sep Purif Technol* 147:62–81
- Rad LR, Irani M, Anbia M (2024) Membrane filtration and adsorption of doxorubicin hydrochloride and fluoxetine hydrochloride from water using polysulfone/MIL-125-NH<sub>2</sub> (Ti) nanofibrous membranes. *J Mol Liq* 408:125429
- Shen Y, Sun P, Ye L, Xu D (2023) Progress of an anaerobic membrane bioreactor in municipal wastewater treatment. *Sci Adv Mater* 15:1277–1298
- Sima X-F, Wang Y-Y, Shen X-C, Jing X-R, Tian L-J, Yu H-Q, Jiang H (2017) Robust biochar-assisted alleviation of membrane fouling in MBRs by indirect mechanism. *Sep Purif Technol* 184:195–204
- Tiraferrri A, Yip NY, Phillip WA, Schiffman JD, Elimelech M (2011) Relating performance of thin-film composite forward osmosis membranes to support layer formation and structure. *J Membr Sci* 367:340–352
- Utomo DP, Kusworo TD, Kumoro AC, Othman MHD (2023) Developing a versatile and resilient PVDF/CeO<sub>2</sub>@GO-COOH photocatalytic membrane for efficient treatment of antibiotic-contaminated wastewater. *J Water Process Eng* 56:104353
- Vatanpour V, Madaeni SS, Moradian R, Zinadini S, Astinchap B (2012) Novel antibifouling nanofiltration polyethersulfone membrane fabricated from embedding TiO<sub>2</sub> coated multiwalled carbon nanotubes. *Sep Purif Technol* 90:69–82
- Wang Y, Ou R, Ge Q, Wang H, Xu T (2013) Preparation of polyether-sulfone/carbon nanotube substrate for high-performance forward osmosis membrane. *Desalination* 330:70–78
- Wang Z, Tu Q, Zheng S, Urban JJ, Li S, Mi B (2017) Understanding the aqueous stability and filtration capability of MoS<sub>2</sub> membranes. *Nano Lett* 17:7289–7298
- Wang S-Y, Sun X-F, Gao W-J, Wang Y-F, Jiang B-B, Afzal MZ, Song C, Wang S-G (2018) Mitigation of membrane biofouling by d-amino acids: effect of bacterial cell-wall property and d-amino acid type. *Colloids Surf B* 164:20–26
- Wang S-Y, Han D-C, Song C, Li M-N, Afzal MZ, Wang S-G, Sun X-F (2019) Membrane biofouling retardation by zwitterionic peptide and its impact on the bacterial adhesion. *Environ Sci Pollut Res* 26:16674–16681
- Wu Y, Xia Y, Jing X, Cai P, Igalavithana AD, Tang C, Tsang DCW, Ok YS (2020) Recent advances in mitigating membrane biofouling using carbon-based materials. *J Hazard Mater* 382:120976–120976
- Yue R-Y, Guan J, Zhang C-M, Yuan P-C, Liu L-N, Afzal MZ, Wang S-G, Sun X-F (2020) Photoinduced superwetting membranes for separation of oil-in-water emulsions. *Sep Purif Technol* 241:116536
- Zhang L, Jiang S, Jia Y, Zhang M, Guo J (2024) Effects of Na<sup>+</sup>/H<sub>2</sub>O<sub>2</sub> on nitrogen removal and sludge activity: performance and mechanism. *J Environ Chem Eng* 12:113194
- Zhao C, Xu X, Chen J, Yang F (2013) Effect of graphene oxide concentration on the morphologies and antifouling properties of PVDF ultrafiltration membranes. *J Environ Chem Eng* 1:349–354
- Zhen J, Wang Z-B, Ni B-J, Ismail S, El-Baz A, Cui Z, Ni S-Q (2024) Synergistic integration of anammox and endogenous denitrification processes for the simultaneous carbon nitrogen, and phosphorus removal. *Environ Sci Technol* 58(24):10632–10643

**Publisher's Note** Springer Nature remains neutral with regard to jurisdictional claims in published maps and institutional affiliations.